Journal of Breast Cancer

J Breast Cancer 2015 June; 18(2): 112-118 http://dx.doi.org/10.4048/jbc.2015.18.2.112

ORIGINAL ARTICLE

Isocryptotanshinone Induced Apoptosis and Activated MAPK Signaling in Human Breast Cancer MCF-7 Cells

Xuenong Zhang, Weiwei Luo, Wenwen Zhao, Jinjian Lu, Xiuping Chen

State Key Laboratory of Quality Research in Chinese Medicine, Institute of Chinese Medical Sciences, University of Macau, Macao, China

Purpose: Isocryptotanshinone (ICTS) is a natural bioactive product that is isolated from the roots of the widely used medical herb *Salvia miltiorrhiza*. However, few reports exist on the mechanisms underlying the therapeutic effects of ICTS. Here, we report that ICTS has anticancer activity and describe the mechanism underlying this effect. **Methods:** The antiproliferative effect of ICTS was determined using 3-(4,5-dimethyl-2-thiazolyl)-2,5-diphenyl-2-H-tetrazolium bromide (MTT) and clonogenic assays. The effect of ICTS on the cell cycle was measured using flow cytometry. Apoptosis was determined by Hoechst 33342 staining, DNA fragmentation assays, and Western blotting for apoptotic proteins. Finally, the effect of ICTS on mitogen-activated protein kinases (MAPKs) was determined by Western blotting. **Results:** ICTS significantly inhibited proliferation of MCF-7 and MDA-MB-231 human breast cancer cells, HepG2 human liver cancer cells, and A549 human lung cancer cells *in vitro*. Among the tested cell lines, MCF-7 cells showed the highest sensitivity to ICTS. ICTS significantly inhibited colony formation by MCF-7 cells. Furthermore, exposure of MCF-7 cells to ICTS induced cell cycle arrest at the G1 phase and decreased mitochondrial membrane potential. Hoechst 33342 staining and Western blot analysis for apoptotic proteins suggested that ICTS induced apoptosis in MCF-7 cells. In addition, ICTS activated MAPK signaling in MCF-7 cells by inducing time- and concentration-dependent phosphorylation of JNK, ERK, and p38 MAPK. **Conclusion:** Our results suggest that ICTS inhibited MCF-7 cell proliferation by inducing apoptosis and activating MAPK signaling pathways.

Key Words: *Apoptosis, Breast neoplasms, Isocryptotanshinone, Mitogen-activated protein kinases*

INTRODUCTION

Chemotherapy remains one of the most important methods of cancer treatment [1], because it effectively prolongs life expectancy and improves the quality of life of patients with cancer. Traditional herbs and medicinal plants have become important resources for anticancer drug screening and development [2,3]. An array of natural products, including wogonin [4], pancratistatin [5], and obtusaquinone [6], selectively kill cancer cells while showing little or no toxicity to normal cells. *Salvia miltiorrhiza* is a well-known medicinal herb that has been used clinically in China for millennia. In recent years, the anticancer activities of *S. miltiorrhiza* have been recognized and tested. Several tanshinones isolated from *S. miltiorrhiza* have a broad range of anticancer activities *in vitro* and *in vivo* [7].

Isocryptotanshinone (ICTS) (Figure 1A) was first isolated from *S. miltiorrhiza* in 1969 [8]. However, there are few reports on the biological activities of ICTS, despite the established use of *S. miltiorrhiza* in traditional Chinese medicine. Han et al. [9] reported that ICTS and two other tanshinones noncompetitively inhibited the activity of protein tyrosine phosphatase 1B, indicating their potential as treatments for type 2 diabetes. In recent decades, tanshinones have been widely investigated for their anticancer effects [7,10]. Cryptotanshinone (CTS), an important bioactive constituent of *S. miltiorrhiza*, inhibits cancer cell proliferation and induces apoptosis in several types of cancer cells, including MCF-7 human breast cancer cells and HepG2 liver carcinoma cells [11-13]. The structure of ICTS is similar to that of CTS. Herein, we report the results of our investigation of the anticancer activity of ICTS.

Correspondence to: **Xiuping Chen**
State Key Laboratory of Quality Research in Chinese Medicine, Institute of Chinese Medical Sciences, University of Macau, Avenida da Universidade, Taipa, Macau, China
Tel: +853-8822-4679, Fax: +853-2884-1358
E-mail: chenxiu0725@yeah.net

This study was supported by the Science and Technology Development Fund, Macao S.A.R (FDCT) (077/2011/A3) and the Research Fund of University of Macau (MYRG118(Y2-L4)-ICMS13-CXP).

Received: January 2, 2015 **Accepted:** June 5, 2015

http://ejbc.kr | pISSN 1738-6756
eISSN 2092-9900

METHODS

Reagents and antibodies

ICTS (>98%) was purchased from ChemFaces (Wuhan, China) and dissolved in dimethyl sulfoxide (DMSO) to produce a stock solution. A working solution was diluted from the stock solution using cell culture medium. Hoechst 33342 stain, 3-(4, 5-dimethyl-2-thiazolyl)-2, 5-diphenyl-2-H-tetrazolium bromide (MTT), propidium iodide (PI), 5, 5′, 6, 6′-tetrachloro-1, 1′, 3, 3′-tetraethyl-imidacarbocyanine iodide (JC-1), and carbonyl cyanide 3-chlorophenylhydrazone (CCCP) were purchased from Sigma-Aldrich (St. Louis, USA). Crystal violet staining solution and DNA loading buffer were obtained from Beyotime Inc. (Haimen, China). Specific antibodies against Bcl-2, bcl-X protein (Bcl-XL), bcl-2-associated X protein (BAX), bcl-2 homologous antagonist-killer protein (BAK), poly-ADP-ribose polymerase (PARP), caspase-3, caspase-9, phospho-c-Jun N-terminal protein kinase (p-JNK), phospho-extracellular regulated protein kinase 1/2 (p-ERK), phospho-p38 mitogen-activated protein kinase (p-p38), JNK, p38, ERK, glyceraldehyde 3-phosphate dehydrogenase (GAPDH), and related secondary antibodies were purchased from Cell Signaling Technology (Beverly, USA). Radio immunoprecipitation assay (RIPA) lysis buffer was obtained from Santa Cruz Biotechnology Inc. (Santa Cruz, USA).

Cell lines and cell culture

MCF-7 and MDA-MB-231 human breast cancer cells, HepG2 human liver cancer cells, and A549 human lung cancer cells were purchased from American Type Culture Collection (Manassas, USA). Cells were cultured in RPMI 1640 or Dulbecco's modified Eagle's medium (DMEM) (Gibco, Carlsbad, USA) supplemented with 10% fetal bovine serum (Gibco) at 37°C in a humidified atmosphere of 5% CO_2.

Cell viability measurement

Cell viability was measured using the MTT assay. In brief, cells were seeded in 96-well culture plates (5,000 cells per well) and treated with a series of concentrations of ICTS (0–40 μM) for 24 hours. After treatment, cells were incubated with serum-free medium containing MTT (1 mg/mL) for 4 hours, followed by removal of the supernatant and dissolution of the formazan crystals with DMSO. The absorbance of the resulting solution was recorded at 570 nm using a microplate reader (PerkinElmer Inc., Waltham, USA).

Clonogenic assay

Clonogenic assays were performed according to previously described methods [14]. MCF-7 cells in the exponential phase of growth were seeded in 6-well plates at a low density (1,000 cells per well). After complete adhesion, cells were treated with ICTS (0–20 μM) for 24 hours, after which the medium containing the ICTS was replaced with fresh medium. Cells were allowed to grow until visible colonies formed, at which point the cells were fixed with 4% paraformaldehyde and cell colonies were stained with 0.5% crystal violet staining solution.

Cell cycle analysis

PI staining was performed to determine the phase distribution of the DNA content of the cells. MCF-7 cells were treated with ICTS (0–10 μM) for 24 hours. After treatment, cells were harvested and fixed with 70% ethanol overnight at -20°C. The fixed cells were washed with cold phosphate-buffered saline (PBS) and stained with PI staining solution (10 μg/mL of Raze A and 50 μg/mL of PI) at 37°C for 15 minutes in the dark. Cell cycle analyses were performed with a flow cytometer and Cell-Quest software (Becton Dickinson, San Jose, USA).

Hoechst 33342 nuclear staining

MCF-7 cells were seeded in 24-well culture plates and treated with the indicated concentrations of ICTS (0–10 μM) for 24 hours. After treatment, cells were stained with Hoechst 33342 (1 μg/mL) at 37°C for 20 minutes in the dark, washed with PBS, and observed by fluorescence inverted microscopy (IX73; Olympus, Tokyo, Japan).

DNA fragmentation assay

DNA fragmentation assays were performed with the DNA Ladder Extraction Kit with Spin Column (Beyotime, Haimen, China) according to the manufacturer's protocol. MCF-7 cells were treated with the indicated concentrations of ICTS (0–20 μM) for 24 hours, after which genomic DNA was extracted. Next, DNA fragments were separated by gel electrophoresis on a 1% agarose gel. DNA was visualized using ethidium bromide staining and photographed under ultraviolet light.

Detection of mitochondrial membrane potential

Changes in mitochondrial membrane potential (MMP) were measured with JC-1 staining. MCF-7 cells were treated with ICTS (20 μM) for 0, 2, 4, 8, or 20 hours. The cells were collected and stained with JC-1 working solution (10 μg/mL) at 37°C for 20 minutes in the dark. The stained cells were analyzed with a flow cytometer (Becton Dickinson). Cells treated with CCCP (10 μM) for 20 minutes were used as the positive control group.

Western blot analysis

Protein expression was determined in MCF-7 cells using

Western blotting according to standard procedures. Briefly, total protein from untreated or treated cells was extracted in RIPA lysis buffer. Equivalent amounts of protein (30 μg) from each group were separated with sodium dodecyl sulfate polyacrylamide gel electrophoresis and transferred onto a polyvinylidene fluoride membrane (Bio-Rad Laboratories, Hercules, USA). After blocking with 5% nonfat milk at room temperature for 1 hour, each membrane was incubated with a specific primary antibody (1:1,000) at 4°C overnight. After three washes in washing buffer (20 mM Tris-HCl, 500 mM NaCl, and 0.1% Tween 20), each membrane was incubated with the appropriate secondary antibody at room temperature for 2 hours. Specific protein bands were visualized using an ECL Advanced Western Blot Detection Kit (Thermo Fisher, Waltham, USA).

Statistical analysis

Data are expressed as mean ± standard deviation from three independent experiments. Significant differences between groups were identified by one-way analysis of variance with Tukey's post hoc test. Results of $p < 0.05$ were considered to be significant. Statistical analyses were performed using GraphPad Prism 5 software (GraphPad Software Inc., San Diego, USA).

RESULTS

Isocryptotanshinone's cytotoxicity

MCF-7, MDA-MB-231, HepG2, and A549 cells were subjected to the MTT assay to evaluate the cytotoxicity of ICTS treatment by measuring cell viability. ICTS significantly inhibited the proliferation of MCF-7, MDA-MB-231, HepG2, and A549 cells in a concentration-dependent manner (Figure 1B). MCF-7 cells showed the highest sensitivity to ICTS. The half-maximal inhibitory concentration of ICTS in MCF-7 cells was about 12.5 μM after 24 hours of treatment. As shown in Figure 1C, morphological changes were observed after exposure to 5–20 μM of ICTS for 24 hours. Moreover, the clonogenic

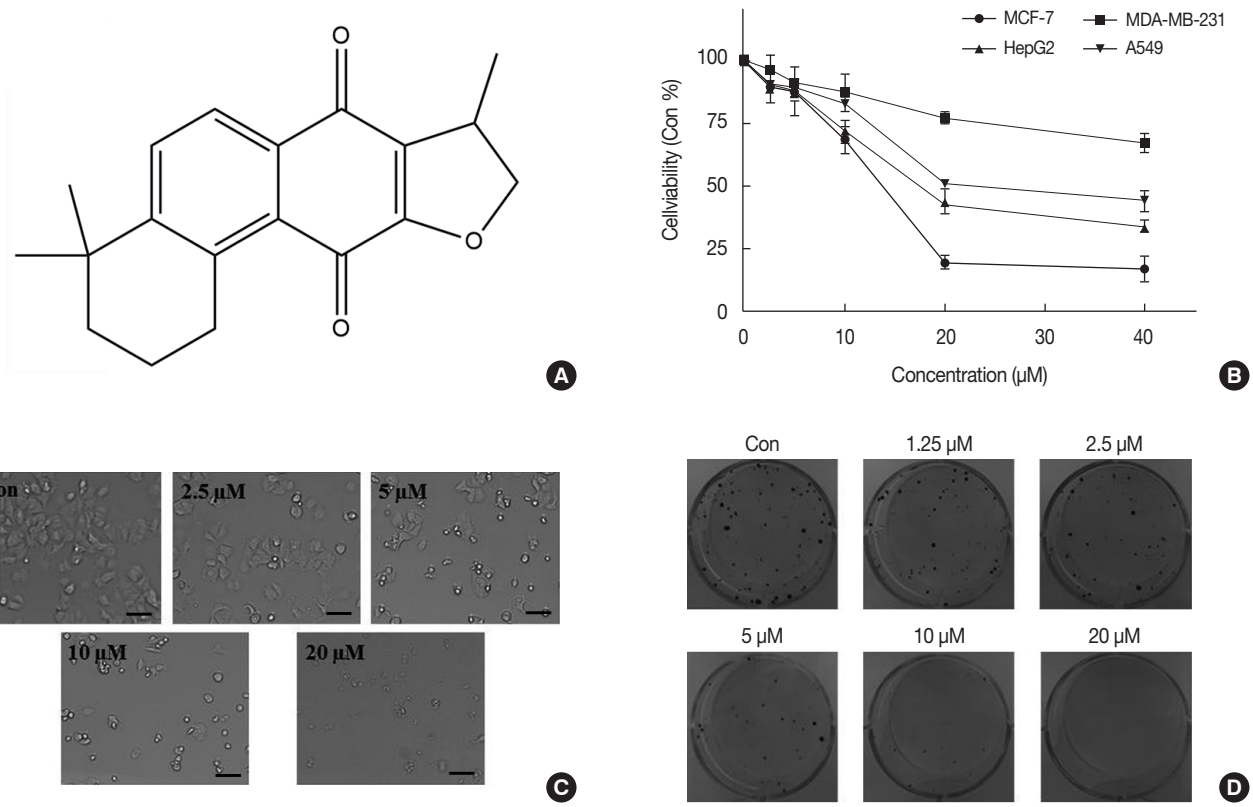

Figure 1. The chemical structure and cytotoxicity of isocryptotanshinone (ICTS). (A) The chemical structure of ICTS. (B) MCF-7, MDA-MB-231, HepG2, and A549 cells were treated with indicated concentrations (0–40 μM) of ICTS for 24 hours. Cell viabilities were measured by 3-(4,5-dimethyl-2-thiazolyl)-2,5-diphenyl-2-H-tetrazolium bromide (MTT) assay. (C) After treatment with ICTS (0–20 μM) for 24 hours, morphological changes of MCF-7 cells were photographed. (D) MCF-7 cells were treated with indicated concentrations of ICTS for 24 hours. At a concentration of 20 μM, ICTS almost completely inhibited colony formation by MCF-7 cells.

http://dx.doi.org/10.4048/jbc.2015.18.2.112

assay showed that ICTS treatment resulted in a remarkable decrease in MCF-7 cell colony number in comparison with untreated MCF-7 cells. At a concentration of 20 μM, ICTS almost completely inhibited colony formation by MCF-7 cells (Figure 1D).

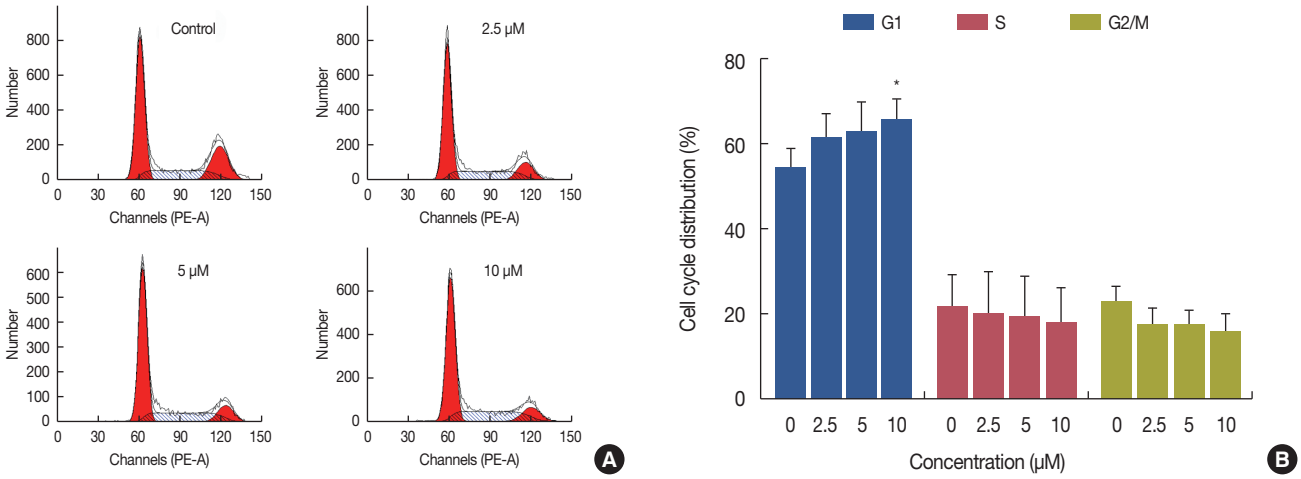

Figure 2. Effect of isocryptotanshinone (ICTS) on cell cycle distribution of MCF-7 cells. (A) Cells were treated with ICTS (0–10 μM) for 24 hours, and cell cycle distribution was analyzed using flow cytometer. (B) The percentages of each G1, S, and G2/M phase for different treatment.
*$p<0.05$ compared with control group.

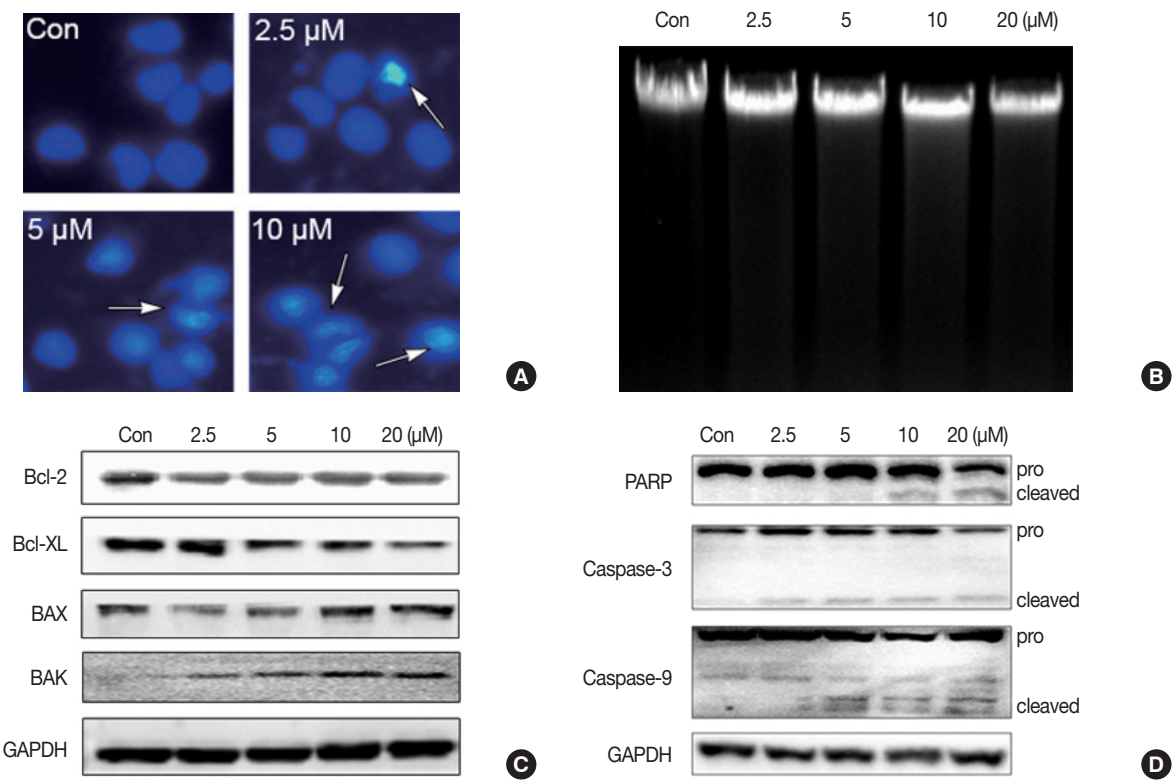

Figure 3. Isocryptotanshinone (ICTS) induced apoptosis in MCF-7 cells. (A) Cells were treated with indicated concentrations of ICTS for 24 hours, and the nuclei were stained by Hoechst 33342. Arrows indicated the condensed nuclei in cells. (B) DNA fragmentation assay was performed in MCF-7 cells after treatment with indicated concentrations of ICTS for 24 hours. (C, D) MCF-7 cells were treated with ICTS (0–20 μM) for 24 hours, and the expressions of Bcl-2, Bcl-XL, BAK, and BAX, as well as poly-ADP-ribose polymerase (PARP), caspase-3, and caspase-9 were detected by Western blot. GAPDH = glyceraldehyde 3-phosphate dehydrogenase.

Isocryptotanshinone induced G1 phase cell cycle arrest in MCF-7 cells

The cell cycle distribution was determined by analysis of DNA content using PI staining. Figure 2A shows the cell cycle distribution of MCF-7 cells treated with ICTS (0–10 μM). The percentages of cells in the G1, S, and G2/M phases following treatment with different concentrations of ICTS were calculated (Figure 2B). G1 phase cell cycle arrest was observed in ICTS-treated cells. The group treated with 10 μM ICTS showed a significant increase in the proportion of G1 phase cells in comparison with the control group ($p<0.05$) (Figure 2B).

Isocryptotanshinone induced apoptosis in MCF-7 cells

To determine whether ICTS induced apoptosis in MCF-7 cells, nuclear fluorescent staining and DNA fragmentation assays were conducted. As shown in Figure 3A, after treatment with ICTS, morphological characteristics indicative of apoptotic cells, including nuclear condensation and fragmentation, were observed in Hoechst 33342-stained MCF-7 cells. Although the DNA fragmentation assay did not show clear "DNA ladders," diffuse fragmentation was observed (Figure 3B). Furthermore, expression levels of apoptosis-related proteins were determined. As shown in Figure 3C, after ICTS treatment, the abundance of antiapoptotic proteins Bcl-2 and Bcl-XL decreased, while that of proapoptotic proteins BAX and BAK increased. In addition, a remarkable increase in the abundance of cleaved PARP, cleaved caspase-3, and caspase-9 was also detected after ICTS treatment (Figure 3D). These results confirmed that ICTS induced apoptosis in MCF-7 cells.

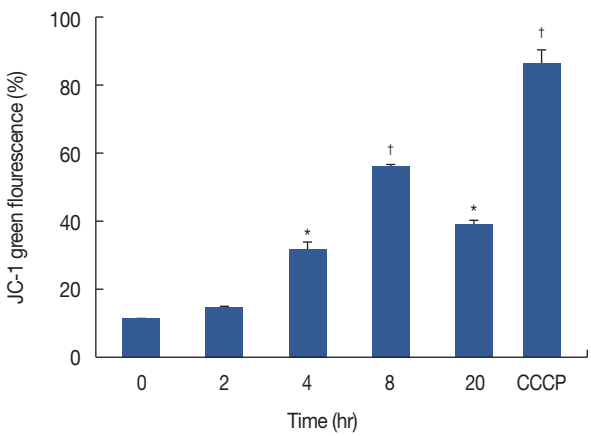

Figure 4. Effect of isocryptotanshinone (ICTS) on mitochondrial membrane potential (MMP). MCF-7 cells were treated with 20 μM ICTS for 0, 2, 4, 8, and 20 hours, the MMP was determined by flow cytometer using JC-1 staining. Cells treated with 10 μM carbonyl cyanide 3-chlorophenylhydrazone (CCCP) for 20 minutes were used as the positive control.
*$p<0.05$; †$p<0.01$ compared with 0 hour treatment group.

Isocryptotanshinone decreased MMP in MCF-7 cells

Decreased MMP is an important characteristic of early apoptosis. To investigate whether mitochondria were involved in ICTS-induced apoptosis, we measured MMP in MCF-7 cells by flow cytometry using JC-1 staining. As shown in Figure 4, MCF-7 cells treated with 20 μM of ICTS showed a time-dependent loss of MMP. As expected, the positive control treatment CCCP (10 μM) resulted in a significant decrease in MMP.

Isocryptotanshinone activated MAPKs signaling in MCF-7 cells

Activation of MAPK signaling pathways is involved in the antiproliferative and proapoptotic effects of chemotherapeutics in many kinds of cancer cells [11,15-17]. We measured activation of JNK, ERK, and p38 in MCF-7 cells after ICTS treatment. As shown in Figure 5, ICTS induced phosphorylation of JNK (p-JNK), ERK (p-ERK), and p38 (p-p38) in MCF-7 cells without affecting total JNK, ERK, or p38. Furthermore, a time-dependent increase in phosphorylation of JNK, ERK, and p38 was observed after treatment with 10 μM ICTS (Figure 5B).

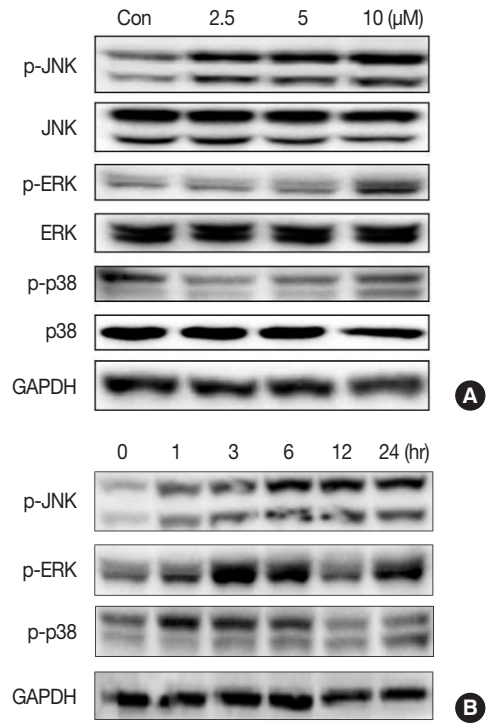

Figure 5. Effect of isocryptotanshinone (ICTS) on the mitogen activated protein kinases signaling. (A) MCF-7 cells were treated with indicated concentrations of ICTS for 24 hours, and the expressions of total and phosphorylated JNK, ERK, p38 were detected by Western blot. Glyceraldehyde 3-phosphate dehydrogenase (GAPDH) was used as internal control. (B) Cells were treated with ICTS for 0, 1, 3, 6, 12, and 24 hours, respectively, the expressions of p-JNK, p-ERK, and p-p38 were detected by Western blot. GAPDH was used as internal control.

http://dx.doi.org/10.4048/jbc.2015.18.2.112

DISCUSSION

Several tanshinones isolated from *S. miltiorrhiza*, including tanshinone I, tanshinone IIA, CTS, and dihydrotanshinone I, inhibit the growth of various human cancer cell lines through antiproliferative (e.g., cell cycle arrest) and proapoptotic effects [7,10]. CTS inhibits proliferation and induces apoptosis in several cancer cell lines, including human liver cancer cells [18], prostate cancer cells [17,19], leukemia cells [20], glioma cells [21], breast cancer cells [22], and lung cancer cells [23]. The structure of the tanshinone ICTS is similar to that of CTS. However, the biological activities of ICTS, especially its anticancer activities, have not been studied extensively. Here, we provide evidence that ICTS possesses potent anticancer effect *in vitro*. ICTS significantly inhibited the proliferation of human breast, liver, and lung cancer cell lines *in vitro*. Among the tested cell lines, the MCF-7 human breast cancer cell line was most sensitive to ICTS, while the MDA-MB-231 breast cancer cell line was least sensitive to ICTS, suggesting that ICTS might be more effective against estrogen receptor positive cancer cells.

Induction of cell cycle arrest and apoptosis are the most important mechanisms of anticancer compounds. Previous studies reported that CTS induced G1 and G1-G0 cell cycle arrest in HepG2 cells [13], multidrug resistant human chronic myeloid leukemia cells (K562/ADM) [20], and two melanoma cell lines [24]. Similar to these reports, we found that ICTS induced cell cycle arrest at the G1 phase in MCF-7 cells; however, the mechanism underlying this effect remains to be identified. Hoechst 33342 staining of MCF-7 cells following ICTS treatment showed morphological characteristics of apoptosis. Although the DNA fragmentation assay did not show a clear "DNA ladder," changes indicative of DNA fragmentation were obvious. Members of the Bcl-2 family, including anti- and proapoptotic regulators, play key roles in cell survival and oncogenesis [25]. Some tanshinones induce apoptosis in cancer cells by regulating Bcl-2 family members. For example, tanshinone IIA increased the Bax/Bcl-2 ratio in H146 lung cancer cells, inhibiting cell growth [26]. CTS induced Fas-mediated apoptosis by upregulating expression of Bcl-2 and MAPK [17], while tanshinone I induced apoptosis in MCF-7 and MDA-MB-231 cells by regulating expression of Bcl-2 and BAX [27]. In the present study, antiapoptotic proteins Bcl-2 and Bcl-XL were downregulated by ICTS, while proapoptotic proteins BAK and BAX were upregulated by ICTS, suggesting that ICTS increased expression of Bcl-2 family members in MCF-7 cells. Bcl-2 family proteins also regulate mitochondrial outer membrane permeability. A loss of MMP can result in the release of several apoptogenic factors into the cytoplasm [28]. We observed a reduction in MMP in ICTS-treated MCF-7 cells. Caspase family proteins are executors of apoptosis [29]. Here, we found that cleavage of PARP, caspase-3, and caspase-9 significantly increased in ICTS-treated MCF-7 cells. Taken together, these results demonstrated clearly that ICTS induced apoptosis in MCF-7 cells.

Signaling by MAPKs, including JNK, ERK1/2, and p38, plays a critical role in the regulation of cell proliferation, differentiation, and apoptosis [11,15-17]. It has been reported that MAPK signaling is involved in the anticancer and proapoptotic activities of many tanshinones. For example, JNK and p38 participate in the effect of CTS on DU145 human prostate cancer cells [11,17], while p38 participates in the effects of dihydrotanshinone and tanshinone IIA on HepG2 liver cancer cells [18] and ovarian cancer cells [16], respectively. The effects of JNK, ERK and p38 activation depend on the stimulus and duration of activation, as well as cell type. Stress-activated MAPKs vary in different cancer cells and play key roles in sensitivity to drug therapy and therapeutic outcomes [30]. Chen et al. [11] reported that CTS activated p38/JNK in DU145 cancer cells, but inhibited ERK. In the present study, we demonstrated that ICTS activated JNK signaling in a concentration- and time-dependent manner, while also activating ERK and p38 signaling, in MCF-7 cells. However, further investigation is required to determine the roles of JNK, ERK, and p38 in inhibition of MCF-7 cell proliferation by ICTS.

The present study showed that ICTS, a natural product isolated from *S. miltiorrhiza*, inhibited proliferation and induced G1 cell cycle arrest and apoptosis in MCF-7 cells. Our findings provide confirmation of the anticancer activities of the traditional Chinese medicine *S. miltiorrhiza*.

CONFLICT OF INTEREST

The authors declare that they have no competing interests.

REFERENCES

1. Chaveli-López B. Oral toxicity produced by chemotherapy: a systematic review. J Clin Exp Dent 2014;6:e81-90.
2. Saha SK, Khuda-Bukhsh AR. Molecular approaches towards development of purified natural products and their structurally known derivatives as efficient anti-cancer drugs: current trends. Eur J Pharmacol 2013;714:239-48.
3. Tan W, Lu J, Huang M, Li Y, Chen M, Wu G, et al. Anti-cancer natural products isolated from Chinese medicinal herbs. Chin Med 2011;6:27.
4. Himeji M, Ohtsuki T, Fukazawa H, Tanaka M, Yazaki S, Ui S, et al. Difference of growth-inhibitory effect of Scutellaria baicalensis-producing flavonoid wogonin among human cancer cells and normal diploid cell. Cancer Lett 2007;245:269-74.

5. Griffin C, Karnik A, McNulty J, Pandey S. Pancratistatin selectively targets cancer cell mitochondria and reduces growth of human colon tumor xenografts. Mol Cancer Ther 2011;10:57-68.
6. Badr CE, Van Hoppe S, Dumbuya H, Tjon-Kon-Fat LA, Tannous BA. Targeting cancer cells with the natural compound obtusaquinone. J Natl Cancer Inst 2013;105:643-53.
7. Zhang Y, Jiang P, Ye M, Kim SH, Jiang C, Lü J. Tanshinones: sources, pharmacokinetics and anti-cancer activities. Int J Mol Sci 2012;13:13621-66.
8. Kakisawa H, Hayashi T, Yamazaki T. Structures of isotanshinones. Tetrahedron Lett 1969;10:301-4.
9. Han YM, Oh H, Na M, Kim BS, Oh WK, Kim BY, et al. PTP1B inhibitory effect of abietane diterpenes isolated from Salvia miltiorrhiza. Biol Pharm Bull 2005;28:1795-7.
10. Chen X, Guo J, Bao J, Lu J, Wang Y. The anticancer properties of Salvia miltiorrhiza Bunge (Danshen): a systematic review. Med Res Rev 2014;34:768-94.
11. Chen W, Liu L, Luo Y, Odaka Y, Awate S, Zhou H, et al. Cryptotanshinone activates p38/JNK and inhibits Erk1/2 leading to caspase-independent cell death in tumor cells. Cancer Prev Res (Phila) 2012;5:778-87.
12. Park IJ, Kim MJ, Park OJ, Choe W, Kang I, Kim SS, et al. Cryptotanshinone induces ER stress-mediated apoptosis in HepG2 and MCF7 cells. Apoptosis 2012;17:248-57.
13. Park IJ, Yang WK, Nam SH, Hong J, Yang KR, Kim J, et al. Cryptotanshinone induces G1 cell cycle arrest and autophagic cell death by activating the AMP-activated protein kinase signal pathway in HepG2 hepatoma. Apoptosis 2014;19:615-28.
14. Wei H, Zhang X, Wu G, Yang X, Pan S, Wang Y, et al. Chalcone derivatives from the fern Cyclosorus parasiticus and their anti-proliferative activity. Food Chem Toxicol 2013;60:147-52.
15. Glassmann A, Reichmann K, Scheffler B, Glas M, Veit N, Probstmeier R. Pharmacological targeting of the constitutively activated MEK/MAPK-dependent signaling pathway in glioma cells inhibits cell proliferation and migration. Int J Oncol 2011;39:1567-75.
16. Jiao JW, Wen F. Tanshinone IIA acts via p38 MAPK to induce apoptosis and the down-regulation of ERCC1 and lung-resistance protein in cisplatin-resistant ovarian cancer cells. Oncol Rep 2011;25:781-8.
17. Park IJ, Kim MJ, Park OJ, Park MG, Choe W, Kang I, et al. Cryptotanshinone sensitizes DU145 prostate cancer cells to Fas(APO1/CD95)-mediated apoptosis through Bcl-2 and MAPK regulation. Cancer Lett 2010;298:88-98.
18. Lee WY, Liu KW, Yeung JH. Reactive oxygen species-mediated kinase activation by dihydrotanshinone in tanshinones-induced apoptosis in HepG2 cells. Cancer Lett 2009;285:46-57.
19. Shin DS, Kim HN, Shin KD, Yoon YJ, Kim SJ, Han DC, et al. Cryptotanshinone inhibits constitutive signal transducer and activator of transcription 3 function through blocking the dimerization in DU145 prostate cancer cells. Cancer Res 2009;69:193-202.
20. Ge Y, Cheng R, Zhou Y, Shen J, Peng L, Xu X, et al. Cryptotanshinone induces cell cycle arrest and apoptosis of multidrug resistant human chronic myeloid leukemia cells by inhibiting the activity of eukaryotic initiation factor 4E. Mol Cell Biochem 2012;368:17-25.
21. Lu L, Li C, Li D, Wang Y, Zhou C, Shao W, et al. Cryptotanshinone inhibits human glioma cell proliferation by suppressing STAT3 signaling. Mol Cell Biochem 2013;381:273-82.
22. Zhou J, Xu XZ, Hu YR, Hu AR, Zhu CL, Gao GS. Cryptotanshinone induces inhibition of breast tumor growth by cytotoxic CD4+ T cells through the JAK2/STAT4/ perforin pathway. Asian Pac J Cancer Prev 2014;15:2439-45.
23. Chen L, Wang HJ, Xie W, Yao Y, Zhang YS, Wang H. Cryptotanshinone inhibits lung tumorigenesis and induces apoptosis in cancer cells in vitro and in vivo. Mol Med Rep 2014;9:2447-52.
24. Chen L, Zheng SZ, Sun ZG, Wang AY, Huang CH, Punchard NA, et al. Cryptotanshinone has diverse effects on cell cycle events in melanoma cell lines with different metastatic capacity. Cancer Chemother Pharmacol 2011;68:17-27.
25. Cory S, Huang DC, Adams JM. The Bcl-2 family: roles in cell survival and oncogenesis. Oncogene 2003;22:8590-607.
26. Cheng CY, Su CC. Tanshinone IIA may inhibit the growth of small cell lung cancer H146 cells by up-regulating the Bax/Bcl-2 ratio and decreasing mitochondrial membrane potential. Mol Med Rep 2010;3:645-50.
27. Nizamutdinova IT, Lee GW, Son KH, Jeon SJ, Kang SS, Kim YS, et al. Tanshinone I effectively induces apoptosis in estrogen receptor-positive (MCF-7) and estrogen receptor-negative (MDA-MB-231) breast cancer cells. Int J Oncol 2008;33:485-91.
28. Tsujimoto Y, Shimizu S. Role of the mitochondrial membrane permeability transition in cell death. Apoptosis 2007;12:835-40.
29. Ola MS, Nawaz M, Ahsan H. Role of Bcl-2 family proteins and caspases in the regulation of apoptosis. Mol Cell Biochem 2011;351:41-58.
30. Sui X, Kong N, Ye L, Han W, Zhou J, Zhang Q, et al. p38 and JNK MAPK pathways control the balance of apoptosis and autophagy in response to chemotherapeutic agents. Cancer Lett 2014;344:174-9.

http://dx.doi.org/10.4048/jbc.2015.18.2.112